Silicon (2022) 14:2051–2065
https://doi.org/10.1007/s12633-021-00996-7

ORIGINAL PAPER

Investigations on Mechanical and Sliding Wear Performance of AA7075 - SiC/Marble Dust/Graphite Hybrid Alloy Composites Using Hybrid ENTROPY -VIKOR Method

Ashiwani Kumar[1] · Mukesh Kumar[2] · Bhavna Pandey[3]

Received: 5 November 2020 / Accepted: 29 January 2021 / Published online: 13 February 2021

Abstract
In this work, AA7075 SiC (0–8 wt.% @ step of 2%) / marble dust (8–0 wt.% @ step of 2%) / graphite (3 wt.%) hybrid alloy composites have been designed and fabricated via high vacuum casting method as per standard procedure, leading to five samples namely SM-08, SM-26, SM-44, SM-62, SM-80 respectively. Thereafter, possible synergistic impact of the complementary combination of SiC/marble dust reinforcing particulates on physical, mechanical, and sliding wear performance of hybrid alloy composites were investigated followed by surface morphology studies. Taguchi approach has been used for sliding wear parametric optimization and hybrid ENTROPY-VIKOR decision-making technique is used for ranking of material based on performance measures. It is observed that with the reinforcing phase the properties like wear performance, coefficient of friction, density, voids content, compressive strength, and impact strength of composites increases considerably while flexural strength diminishes. Thus, SM-62 alloy composite (having 6 wt.% SiC, and 2 wt.% marble dust) shows better improved overall performance relative to others.

Keywords AA7075 · Hybrid ENTROPY –VIKOR · Taguchi method · Sliding wear · SiC · Marble dust · Graphite · Alloy composites

1 Introduction

AA7075 alloys play an important role in different technological areas like automotive and aerospace sectors owing to their superior strength to weight ratio and other mechanical and tribological properties. AA7075 alloys show the low resistance to sliding wear performance under dry and lubrication condition. Available various accessible grades of some alloys, AA7075 alloy having present in various element trend to show good mechanical properties that develop and researcher can be utilized for tribological application. The ceramic based composite performance can be increased with increase in ceramic particulates and also improve the wear resistance and friction. To enhance their wear properties aluminium alloy SiC/MD/Gr filled composites are being explored.Many materialist /scientists are reported that increase the ceramic particulate with tribological and mechanical performance increase also [1, 2]. Chen et al. [3] examined the mechanical characteristics of silicon carbide and tungsten carbide and obtained the tensile strength, plasticity and hardness of composites enhances whereas ductility reduces. Prabu et al. [4] analysis of mechanical performance of SiC filled AA7075 alloy composite and found the compressive strength and hardness of fabricated composites rise with increment in SiC. Kumar et al. [5] analyzed the influence of Ni particulate on mechanical and tribological characterization of AA7075 alloy composite and found the flexural strength, hardness, compressive strength, impact strength and wear resistance of composites improve with present in Ni content. Ravi et al. [6] evaluation of mechanical properties of TiC /AA7075 based composite and noticed that the micro hardness of composite rise with increment in TiC particulate and also particle size reduces. Alhawari et al. [7] analyzed of the tribological properties of Al_2O_3

✉ Ashiwani Kumar
ashi15031985@gmail.com

[1] Mechanical Engineering Department, Feroze Gandhi Inst. of Engg.& Tech, Raebareli, U.P. 229316, India

[2] Mechanical Engineering Department, Malaviya National Inst. of Tech, Jaipur, Rajasthan 302017, India

[3] Mechanical Engineering Department, Chartered Institute of Technology, Sirohi, Rajasthan 307510, India

particulate filled AA356 composite and noticed it reduce in the wear rate with increment in Al_2O_3 content. Kiran et al. [8] examined of the influence of SiC/Al_2O_3 on the wear behavior of AA6061 hybrid composite and reported the wear resistance enhances with growing in the particulate content. Kumar and Kumar [9] analyzed effect of B_4C/ Rice rush on mechanical and sliding performance of AA7075 composite and found that various characterizations like hardness, compressive strength, tensile strength and flexural strength and wear resistance of composite increases with an increase the B_4C/rice rush particulates. Bhaskar et al. [10] evaluated the material performance of AA2024/SiC alloy composite is determined via MCDM methods like (AHP; TOPSIS) and found that outcomes are in tune with the raking performance of designed composite. Kumar and Kumar [11] investigated that the optimization of stir casting processing parameters of SiO_2/SiC/AA2024 composite by using the Taguchi and PSI Method. In the previous year studies, the different multi decision criteria, methods are implemented to investigate the optimization problem of composite [12, 13]. The various scientists/ researchers have developed the different techniques like TOPSIS, PSI Method [14, 15]. The preference selection index (PSI) optimization method is effectively applied to a distinct area like Engineering and Management [16–19]. Thus, in the present investigations are-

(i) Design and developed of Silicon carbide /Marble dust /Graphite particulate reinforced based AA7075 hybrid alloy composite.
(ii) Evaluation of mechanical and tribological performance of Silicon carbide /Marble dust /Graphite particulate filled AA7075 hybrid alloy composite.
(iii) The ranking material performance of composites was analyzed via Taguchi and hybrid ENTROPY-VIKOR Method.

Abbreviations

AA7075: Aluminum alloy composite
SiC: Silicon carbide
MD: Marble dust
Gr: Graphite
Hybrid ENTROPY–VIKOR: Hybrid ENTROPY - VIseKriterijumskaOptimizacija I KompromisnoResenj
SM: Silicon carbide and Marble dust

2 Experimental Procedures

2.1 Details of Materials and Fabrication Method

The materials,design aspects and fabrication method of silicon carbide /marble dust /graphite filled aluminum alloy composite details (Table 1) and Fig. 1a, b and c are given in a particular section.

Table 1 Chemical composition of Marble dust

Oxides compound	CaO	Al_2O_3	SiO_2	Fe_2O_3	MgO
Percentage	42.45	0.520	26.35	9.40	1.52

Details of Materials:

The particular base material(AA7075 alloy) matrix in the form of rods (8 mm diameter) delivered by Bharat aerospace metals Mumbai India and the chemical composition are Zinc (~5.5 wt.%), Copper (~1.6 wt.%), Magnesium (~2.5 wt.%), Iron (~0.5 wt.%), Silicon (~0.4 wt.%), Manganese (~0.3 wt.%), Titanium (~0.2 wt.%), Chromium (~0.15 wt.%) and Aluminum rest wt.%.
Graphite reinforcement is delivered by Savita Scientific Pvt. Ltd. Jaipur; particle size of 97.5 μm.
Marble dust (MD) and Silicon Carbide (SiC) are delivered by Savita Scientific Pvt. Ltd. Jaipur, India; particle size of 20 μm [6].

Composition of Al7075/SiC/Gr/MD hybrid alloy composite

SM-0 8 (0 wt.% of SiC; fixed 3 wt.% of Gr and 8 wt.% of MD; rest AA7075 alloy)
SM-26 (2 wt.% of SiC; fixed 3 wt.% of Gr and 6 wt.% of MD; rest AA7075 alloy)
SM-44 (4 wt.% of SiC; fixed 3 wt.% of Gr and 4 wt.% of MD; rest AA7075 alloy)
SM-62 (6 wt.% of SiC; fixed 3 wt.% of Gr and 2 wt.% of MD; rest AA7075 alloy)
SM-80 (8 wt.% of SiC; fixed 3 wt.% of Gr and 0 wt.% of MD; rest AA7075 alloy)

Fabrication method:

The fabrication of silicon carbide/marble dust /graphite filled aluminum alloy composite was manufactured by using the high vacuum casting process as discussed below [7, 20]. The cleaned small pieces of the composite are melted in the vessel of graphite using an electric furnace as per machine standard. The entire material was melted at 860 °C for 25 min after the temperature of the material is dropped to 680 °C. The present impurities in materials were removed with the mixed of flux via mean of formation slag. The ceramic reinforcements are preheated in induction furnace (muffle) at 820 °C for 3 h as per machine stand. After that the increase in wettability of reinforcing material phases in alloy melted with powder (2 weight percentage of Mg) was

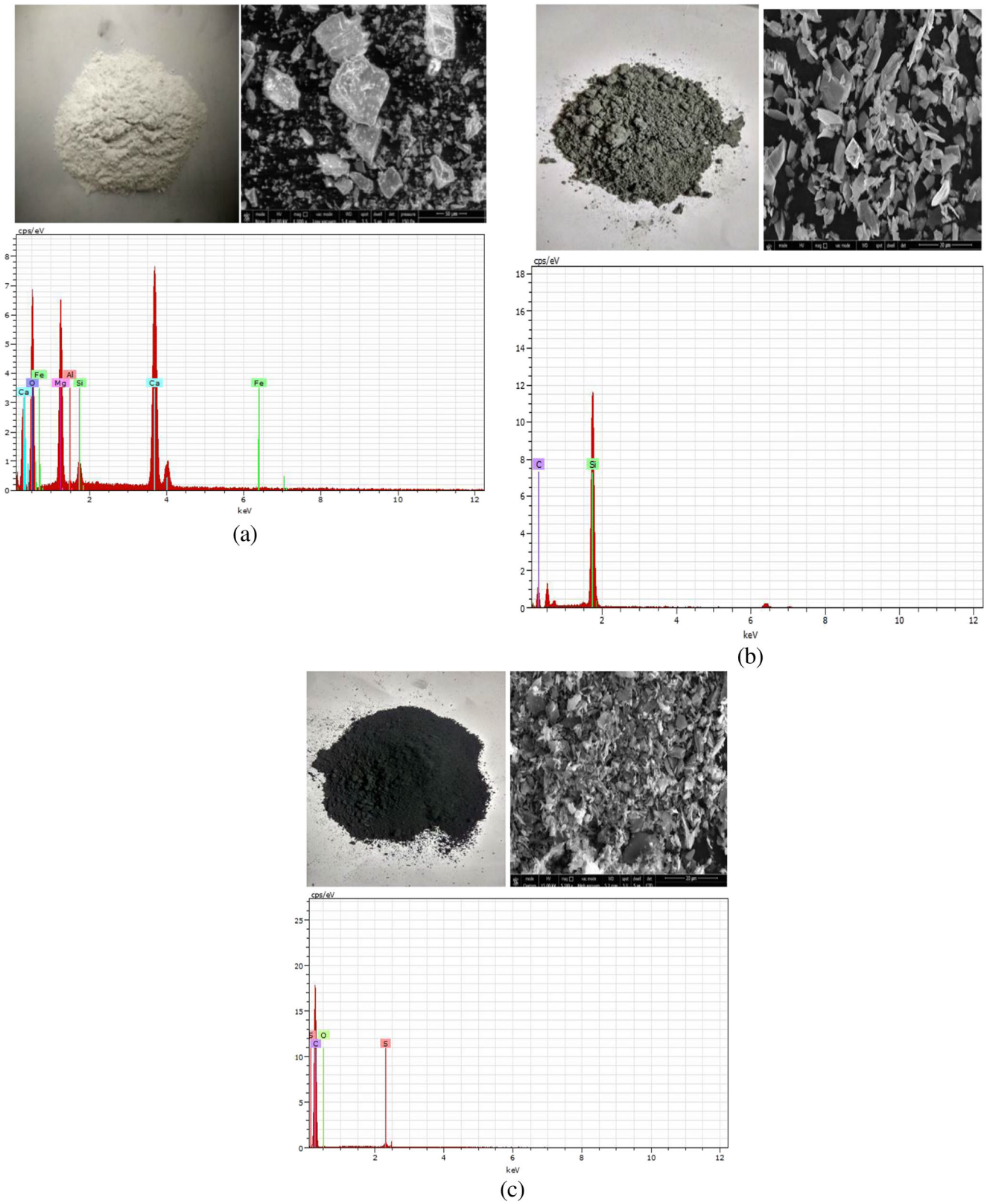

Fig. 1 **a** Marble dust powder with SEM and EDX image **b** Silicon Carbide powder with SEM and EDX image **c** Graphite powder image with SEM and EDX image

mixed and uniform mixing of materials were used via automatic stirrer.The mixture of material was poured into fixed cast iron mould and allowed it to solidify at room temperature in normalizing process for 35 min. Finally, the composite

specimens were prepared through wire EDM equipment as per standard and also used various polishing grade paper. Thus, the prepared specimens are used to perform the physical, mechanical and tribological characterization.

2.2 Physical and Mechanical Characterization

The experimental density(ρ_e) of the experimental sample was measured via using a standard immersion approach following the Archimedes principle as per ASTMD792 [21] while theoretical density (ρ_t) was computed via the rule of mixture approach in Eq. 1, state by Agarwal and Broutman.The voids or porosity of developed composite samples were achieved by Eq. 2 [22].

$$\rho_t = \frac{1}{\frac{W_{Al7075}}{\rho_{Al7075}} + \frac{W_{SiC}}{\rho_{SiC}} + \frac{W_{Gr}}{\rho_{Gr}} + \frac{W_{MD}}{\rho_{MD}}} \tag{1}$$

where W indicates weight fraction of composite and ρ represents density of composite respectively.

$$V = \frac{\rho_t - \rho_e}{\rho_t} \tag{2}$$

The experimental tensile strength sample size was taken as $150 \times 10 \times 10\ mm^3$; dimension of span length = 65 mm; as per standard (ASTMD3039–76) and the experimental tensile strength are achieved through Universal Testing Machine of composite. The similar apparatus is utilized for computing flexural strength of experimental samples ("size of $127 \times 12.5 \times 4\ mm^3$; experimental length of span =70 mm; as per ASTM D- 2344–84"). The toughness of experimental samples (size of $55 \times 10 \times 10\ mm^3$; experimental angle of notch (45°); depth of sample = 2.5 mm; as per ASTMD-256) were via charpy V-notch experiment method (Impact tester apparatus). The experimental sample of rockwell hardness (dimension of $10 \times 10 \times 75\ mm^3$ as per ASTM E18 is measured via using vicker micro hardness tester and compression strength of experimental specimens (dimensions of $10 \times 10 \times 10\ mm^3$; as per ASTM E9–09) could be determined via Universal Testing Machine [23].

2.3 Sliding Wear Experimental Procedure

The performance of sliding wear experimental specimens were performed on a Pin on disc tribometer (Model TR-20; ASTM G99; DUCOM Bangalore, India) as per standard and are taken input factor as indicated in Table 1. Experimental size of sample was taken $25 \times 10 \times 10\ mm^3$ and experimental apparatus of sliding disc are made of hardened ground steel and machine specifications (as EN:- 31; diameter of experimental disc (165 mm); 8 mm of thickness; hardness of disk(62 HRC); 0.6μRa of surface roughness). The diameter of experimental rotating disk is taken fixed at 50 mm during the entire research work. The surface of rotating disk is neat by using acetone and emery sand grades prior the begin of each experimental run of composite specimens and other apparatus (electronically weight measurement apparatus with an correctness of ±0.001 mg) are operated to obtain the weight loss of experimental specimen and operating software (Win Ducom 2010-V07) was utilized to control the machine parameter [13, 22, 23].The specific wear rate (mm^3/N-m) of experimental sample are computed by using (Eq. 3).

$$W_S = \frac{\Delta m}{\rho \times V_S \times t \times F} \tag{3}$$

where Δm denotes weight loss of specimen (g), ρ represents density of composite (g/mm^3), t indicates experiment time (s), Vs expresses velocity of sliding (m/s), and F represents normal load of sample (N). Further the SEM microstructure studied that worn surface of specimen is examined by using FESEM equipment (FEINOVA-450). It helps to understand wear mechanism for the performance of sliding wear of hybrid composites throughout the experimental work [20].

2.4 Taguchi and ANOVA Experiment

Taguchi approach is a very significant statistical optimization tool and implemented by various researchers/materialist during the entire the experimental work across the literature review [6, 23].This approach helps to properly understanding of research data and identifying input control factors as (sliding distance; sliding velocity; normal load) during sliding test. It might be affecting the test response and uncontrolled parameters and helps analysis of response with reducing the test trial. Further, it could be validated through ANOVA approach. It computes the optimal variable response and compares the test results confirmation through model. The orthogonal array design is based on permutations and combination concept; achieved the significant variable response. Table 2 shows the combination of level and input control parameters experimental range for research work.

Further, L_{16} orthogonal array concept was utilized for the DOE in place of $4^4 = 256$ runs via design of factorial. The wear rate and COF results are obtained through Eq. 4. Thus,

Table 2 Working range of selected parameters [9, 39]

Control factor	Level					
	I	II	III	IV	V	Unit
Normal load	10	20	30	40	50	N
Filler content	SM-08	SM-26	SM-44	SM-62	SM-80	wt.%
Sliding velocity	0.9	1.4	1.9	2.4	2.9	m/s
Sliding distance	500	750	1000	1250	1500	m

the lower wear rate is achieved by using smaller the better approach (S/N Ratio).

SB (Smaller the better) approach:

$$\frac{S}{N} = -10\log\frac{1}{Q}\sum P^2 \tag{4}$$

where, 'Q' indicates No. of observations; 'P' represents the observed data.

2.5 Hybrid ENTROPY –VIKOR Methodology

Ranking performance of distinct compositions based on different factors was achieved via Hybrid Entropy -VIKOR methodology. Further, Entropy approach was considered for weight measurement while VIKOR approach was used for the alternatives ranking performance. This ranking performance methodology is based on the four main steps (see in Fig. 2).

Step 1: Identifying of alternatives and criterions

Compute the number of alternatives (Ai, i = 1, 2.....u) and criteria (Cj, j = 1, 2.....v) for the given MCDM problem.

Step 2: Preparing the decision matrix: The investigated problem structure is indicated the multi-alternative (say *m*-alternatives) and multi-criteria (say *n*--criteria) and the product of decision matrix is also represented in the form (say matrix D of *m*×*n* order) in Eq. 5

$$\begin{array}{c} \\ D_{m\times n} = \end{array} \begin{array}{c} \begin{matrix} C_1 & C_2 & \cdots & C_n \end{matrix} \\ \begin{matrix} \mathrm{A}_1 \\ \mathrm{A}_2 \\ \vdots \\ \mathrm{A}_m \end{matrix} \begin{bmatrix} p_{11} & p_{12} & \cdots & p_{1n} \\ p_{21} & p_{22} & \cdots & p_{2n} \\ \vdots & \vdots & \ddots & \vdots \\ p_{m1} & p_{m2} & \cdots & p_{mn} \end{bmatrix} \end{array}$$

where $C_1, C_2, \ldots, C_n$ are the $n-$criteria and $\mathrm{A}_1, \mathrm{A}_2, \ldots, \mathrm{A}_m$ are the $m-$alternatives

(5)

Step 3: Evaluating the weight of criteria through Entropy method

Step 1: Estimate the entropy of the j^{th} criterion in the decision matrix by Eq. 6:

$$\mathrm{E}_j = -\varsigma \sum_{j=1}^{N} \rho_{ij} \ln\left(\rho_{ij}\right) \tag{6}$$

$$\rho_{ij} = \frac{x_{ij}}{\sum_{i=1}^{M} x_{ij}}$$

Where k represents constant and an estimate value of $\varsigma = \frac{1}{\ln(P)}$

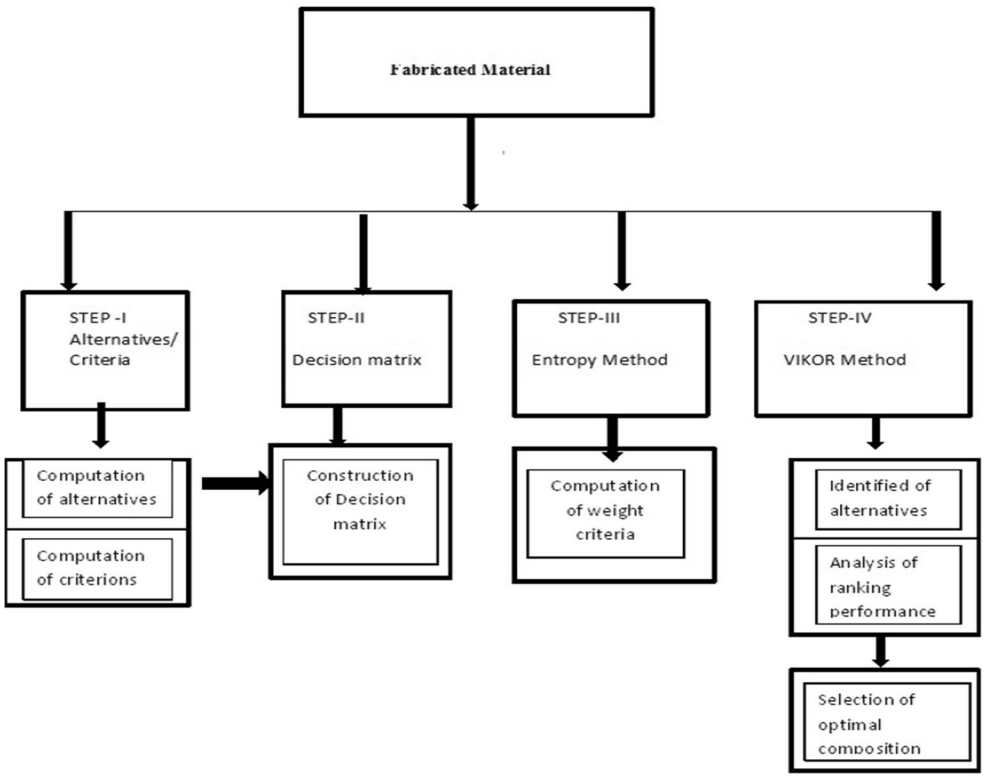

Fig. 2 hierarchy structure of the investigate problem

Step 2: Estimate weight of each criterion via Eq. 7

$$\omega_j = \frac{\psi_j}{\sum_{j=1}^{N} \psi_j} \tag{7}$$

where ψj represents the degree of diversity output for jth criterion and assumed as ψj =1 − Ej.

Step 4: Choosing the best material

The steps followed in the VIKOR optimization technique are as follows:

Step I: To discern the PDCs and alternatives/ options of the research problem then decision matrix is made. P denotes the alternative and Q indicates the defining criteria, then the decision matrix ($_{DP\times Q}$) is made by Eq. 8.

$$D_{P\times Q} = \begin{bmatrix} a_{11}a_{12}\ldots a_{1N} \\ a_{21}a_{22}\ldots a_{2N} \\ \ldots\ldots\ldots\ldots \\ \ldots\ldots\ldots\ldots \\ a_{M1}a_{M2}\ldots a_{MN} \end{bmatrix} \tag{8}$$

Where, an element a_{ij} of the decision matrix $D_{P\times Q}$ represents the actual value of the i^{th} alternative in term of j^{th} PDC.

Step 2: To create the decision matrix,$(z_{ij})_{max}$indicates the benefits and $(z_{ij})_{min}$denotes as cost criterion obtained via Eq. 9

$$\begin{aligned} (Z_{ij})_{max} &= max_{i^{Z_{ij}}} = \max\left[Z_{ij}, i = 1,2 \quad N\right] \\ (Z_{ij})_{min} &= min_{i^{Z_{ij}}} = \min\left[x_{ij}, i = 1,2 \quad N\right] \end{aligned} \tag{9}$$

Step 3: To estimate the utility measure (α_i) and regret measure (β_i) via Eqs. 10 and Eq 11

$$\begin{aligned} \alpha_i &= \sum_{j=1}^{N} \frac{\varpi_j\left[(Z_{ij})_{\max} - Z_{ij}\right]}{\left[(Z_{ij})_{\max} - (Z_{ij})_{\min}\right]}, \textit{if } j \textit{ represents benefits citeria} \\ \alpha_i &= \sum_{j=1}^{N} \frac{\varpi_j\left[Z_{ij} - (Z_j)_{min}\right]}{\left[(Z_{ij})_{max} - (Z_{ij})_{min}\right]}, \textit{if } j \textit{ denote as cost criteria}, \text{ for } j = 1,2 \quad N \end{aligned} \tag{10}$$

$$\beta_i = Max^x of\left\{\frac{\varpi_j\left[(Z_{ij})_{\max} - Z_{ij}\right]}{\left[(Z_{ij})_{\max} - (Z_{ij})_{\min}\right]}\right\}, \text{for j} = 1,2 \quad N \tag{11}$$

Step 4: Finally, VIKOR index (Ω_i) estimated by using Eq. 12

$$\Omega_i = \xi\left(\frac{(\alpha_i - \alpha_i^-)}{(\alpha_i^+ - \alpha_i^-)}\right) + (1-\xi)\left(\frac{(\beta_i - \beta_i^-)}{(\beta_i^+ - \beta_i^-)}\right) \tag{12}$$

Where,

$\alpha_i^+ = {}^{max}\alpha_i = \max[\alpha_i, \ i = 1, \ 2\ldots M]$;

$\alpha_i^- = {}^{min}\alpha_i = \min[\alpha_i, \ i = 1, \ 2\ldots M]$.

$\beta_i^+ = {}^{max}\beta_i = \max[\beta_i, \ i = 1, \ 2\ldots M]$;

$\beta_i^- = {}^{min}\beta_i = \min[\beta_i, \ i = 1, \ 2\ldots M]$.

ξindicates as maximum utility value for weight and $(1-\xi)$ denotesas individual regret for weight and ξvalue is opted as 0.5

Step 5: The all alternatives of VIKOR index value are taken in ascending sequence and the lower value of VIKO index shows the best alternative in allcomposite.

3 Results and Discussion

3.1 Physical and Mechanical Characterization

3.1.1 Effect of Density, Voids Content and Hardness Characterization

The effect of SiC / Marble dust on theoretical density, experimental density, void content and hardness characteristics of SM alloy composites are tatbulated and depicted in Table 3, Fig. 3. It was noticed that theoretical and experimental density shows increasing trend in magnitude. It was observed that the Theoretical density SM alloy composites increases with increment in weight percentage of SiC/marble dust content (MD). It is evident from the Fig. 3 and Table 3, the Theoretical density of composite is 2.89 g/cc at 0 wt.% SM. On the addition of 2 wt.% SM the Theoretical density of alloy composite increases up to range from 2.89–2.90 g/cc); after that theoretical density of composite shows suddenly changed and accelerates (range from 2.90–2.96 g/cc). It was noticed the experimental density of SM alloy composite increase with increment in weight percentage of SiC/marble dust content (MD). It is noticed that from Fig. 3 that the experimental density of the composite of SM alloy composite is 2.84 g/cc at 0 wt.% SM. On the addition of 2 wt.% SM the density of alloy composite decreases up to the range from 2.84–2.80 g/cc); after that the density of composite shows suddenly changed and accelerates (range from 2.80–2.87 g/cc) and SM-80 alloy composite of the density shows increase with increment in weight percentage in filler content. Hence, The density

Table 3 Physical and mechanical characterization

Characteristics	SM-08	SM-26	SM-44	SM-62	SM-80
Experimental density (g/cc)	2.84	2.85	2.86	2,87	2.88
Theoretical density (g/cc)	2.89	2.90	2.92	2.94	2.96
Voids content (%)	1.73	2.39	2.05	2.38	2.70
Hardness (HV)	52	55	59	65	72
Compressive strength(MPa)	400	440	535	645	665
Impact strength (KJ/m^2)	9	10	12	14	17
Flexural strength (MPa)	245	275	335	255	215

increases due to equal presence of harder reinforcing ceramic phase (SiC ~3.21 g/ cc; G r ~ 2.26 g/cc, MD 0.7 g/cc) in the unfilled alloy matrix. This may be attributed that the equal presence of particulate increase the interfacial bonding between base matrix and reinforcement, therefore, minimize the voids present in alloy composite. Similar outcomes are reported by various researchers [37, 38]. Increment in density, enhance in weight percentage of Sic/MD due to the presence of casting metallurgy defect in material. Similar outcomes are reported by different researchers [6, 13, 21, and]. Hence, the theoretical density of SM alloy composite value is always higher than the experimental density. The trend of the both density of the SM alloy composite is SM-08 < SM-26 < SM-44 < SM-62 < SM-80. It was noticed that the voids /porosity content of SM alloy composites increase with increment in weight percentage of SM. Precisely voids/porosity content reduces from 2.39% to 2.05 for SM-26 and SM-44. The voids content of composite reduction happens owing to appropriate dispersion and distribution of particulate into the alloy matrix while remaining composite of void contents value is 2.38, and 2.70%. According to the value of voids content should be acceptable range 0–10% as per industrial standard. The outcome of separation of SM into matrix or owing to air bubbles made through the mixing outcome of improving in voids content of alloy composites. It might be that the maximum porosity leads to little strength interfacial bonding between SiC/MD filled al 7075 alloy composites. The voids content /porosity

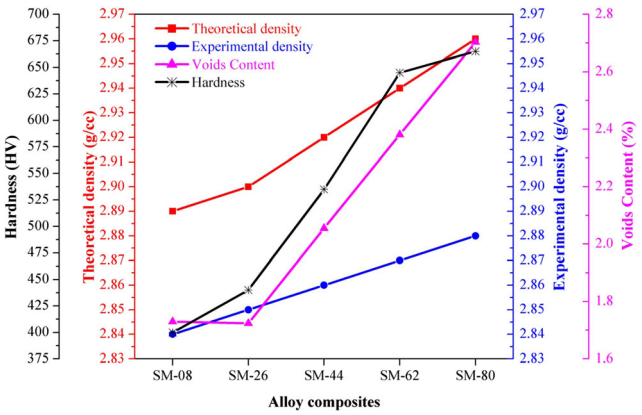

Fig. 3 Effect of density, void content and hardness characterization

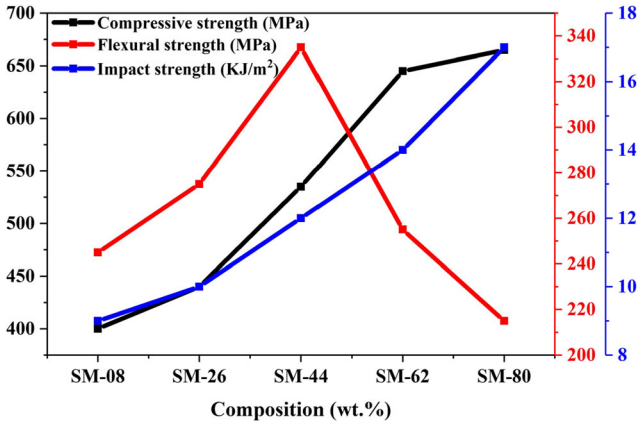

Fig. 4 Mechanical characterization

reduces with improve in hardness of SM composite. The voids content order is SM-08 > SM-44 > SM-62 > SM-26 > SM-80 [6, 21].It is noticed that the hardness of composite increases with enhance in the weight percentage of SiC/MD. The SM-80 alloy composite of hardness value is higher than other composite. The SM alloy composites show linearly increase in hardness of composite. Similar observation is reported by different researchers [13]. Hence, the trend of hardness composite is SM-0 < SM-26 < SM-44 < SM-62 < SM-80. Enhance in hardness owing to the change in plastics deformation and presence of hard ceramic particles of SM alloy composite. A similar trend was observed by different researchers [6, 7] that addition of various particulate like Silicon carbide, Boron carbide and AlB_2 particle enhances in hardness of SM composite. Hence, Hardness of SM alloy composite also improves due to the strength mechanism effect presence in reinforcement and alloy matrix. This may be attributed that the Hardness of composite improves due to increase in the density of reinforcement of particles, dislocation density, particle size and grain size and reduction in the porosity of composite could be enhanced the hardness of composite. Hall-Peach relationship aids to improve the hardness of composite. Similar results are reported by various researchers [31–38].

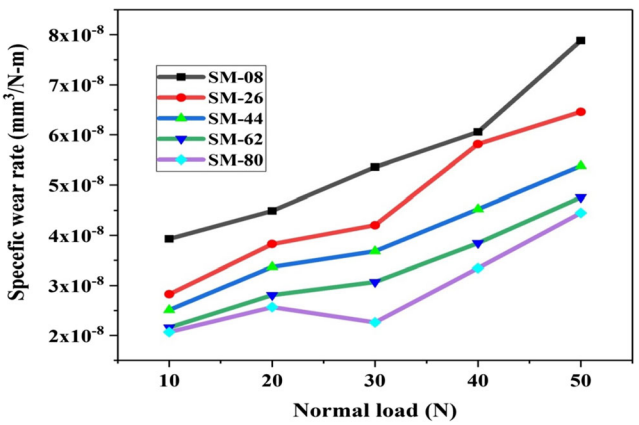

Fig. 5 Effect of normal load on specific wear rate

3.1.2 Mechanical Characterization

The effect of SiC / MD on mechanical characterization like (compressive, flexural and impact strength) of SM alloy composite are depicted in Fig. 4. It was observed that compressive and impact strength of MS alloy composites is enhanced with an enhance in weight percentage of SiC/MD content while the flexural strength reduces with increase in particulate content. It is observed that the compressive strength of a SM alloy composite increase with an increase in weight percentage of SiC/MD and The SM −80 alloy composite of compressive strength is higher while the compressive strength of other compositions are slowly gradually improves with increment in weight percentage of filler content. The improvement of compressive strength may be due to the addition of various fillers like SiC, B_4C, Gr, and Cu powder were reported by other researcher/ scientist. Therefore, it was observed that the compressive strength order as SM-80 > SM-62 > SM-44 > SM-26 > SM-08. Enhance in compressive strength due to the hard ceramic particles, crack growth, dislocation and strengthening the mechanism of AS alloy composite [6, 13]. It is noticed that the impact strength of SM alloy composite increases with increment in weight percentage of SiC/MD. It may be attributed to SM alloy composite is presence in minimum voids while it was higher impact strength for SM-80 and SM-08 alloy composite of impact strength is lower. The similar result is also said by Kumar et al. [7] for SIC/MD particulate mixed Al 7075 metal alloy composite. Hence, the impact strength order is SM-08 < SM -26 < SM-44 < SM-62 < SM-80. Influence in flexural strength while adding the SiC/MD particulates of AA7075 aluminum alloy composites. It is noticed that the flexural strength of SM alloy composite was increased (240 MPa to 330 MPa) with enhancement in weight percentage of SiC/MD while it was suddenly reduced (330 MPa–180 MPa) for SM alloy composite. Similar trends

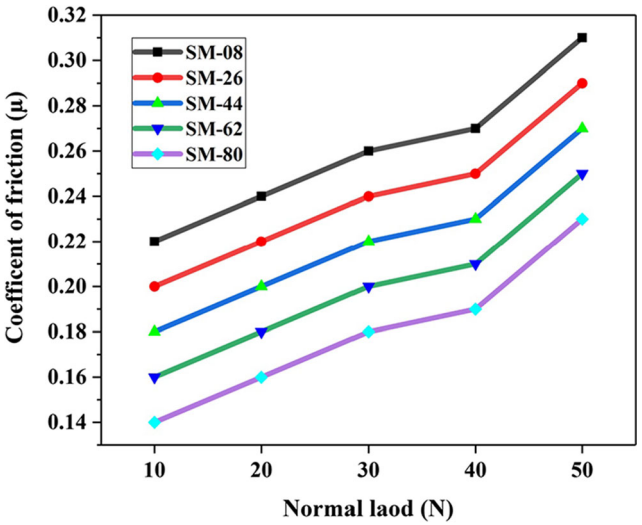

Fig. 6 Effect of normal load on coefficient of friction

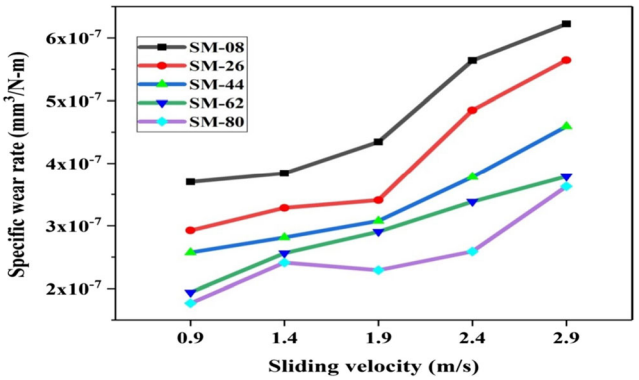

Fig. 7 Effect of sliding velocity on specific wear rate

are reported by different scientists [7, 13] For including the different particulates like SiC, Gr, B_4C, Al_2O_3 etc. and the flexural strength trend is SM −80 < SM-62 < SM-08 < SM-26 < SM-44. Therefore, the flexural strength reduces due to weak bonding and inappropriate distribution in casting method. The reason for the flexural strength composites decreases due to increase crack, propagation and pores in the SM alloy matrix and the outcomes of composites are in excellent agreement with other examination in this particular field [8]. This may be attributed that the SM alloy composites being take equal presence of both ceramic particulate increases good interfacial adhesion between matrix reinforcement, hence minimum void content, thereby strongly load transfer to reinforcing phases in matrix, this results show the few chance of matrix failure. The minimum magnitude of alloy composite shows the presence of voids content that poorly move the flexural load to its filler phase, thus matrix has to sustain more transverse load. The properties of the alloy composite is anisotropic by nature. The interface strength between ingredients of alloy composite may be poor for flexural loading resulting in poor flexural strength for composites having SiC >4 wt.%. The non-uniform distribution of reinforcement and voids content may be the other reasons [37, 38].

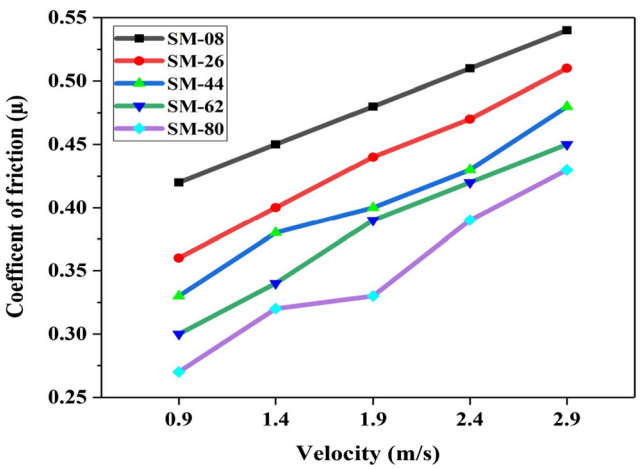

Fig. 8 Effect of sliding velocity on coefficient of friction

Table 4 Experimental layout of L_{25} orthogonal array

Expt. No	Normal load (N)	Filler Content (wt.%)	Sliding Velocity (m/s)	Sliding Distance (m)	Specific wear rate (mm^3/N-m)	S/N Ratio (dB)
1	10	0	0.9	500	0.005268	45.5671
2	10	2	1.4	750	0.008736	41.1737
3	10	4	1.9	1000	0.01768	35.0504
4	10	6	2.4	1250	0.322432	9.8312
5	10	8	2.9	1500	0.044772	26.9799
6	20	0	2.4	500	0.008303	41.6153
7	20	2	2.9	1000	0.023144	32.7112
8	20	4	0.9	1250	0.166035	15.5960
9	20	6	1.4	1500	0.087356	21.1741
10	20	8	1.9	500	0.032288	29.8192
11	30	0	1.4	1000	0.030863	30.2112
12	30	2	1.9	1250	0.042445	27.4435
13	30	4	2.4	1500	0.055196	25.1618
14	30	6	2.9	500	0.012126	38.3256
15	30	8	0.9	750	0.181237	14.8351
16	40	0	2.4	1250	0.00228	52.8413
17	40	2	0.9	1500	0.236007	12.5415
18	40	4	1.4	500	0.030342	30.3591
19	40	6	1.9	750	0.401042	7.9362
20	40	8	2.4	1000	0.074754	22.5273
21	50	0	1.9	1500	0.075146	22.4819
22	50	2	2.4	500	0.009635	40.3230
23	50	4	2.9	750	0.01768	35.0504
24	50	6	0.9	1000	0.243657	12.2644
25	50	8	1.4	1250	0.371614	8.5982

3.2 Wear Experimental Studies

3.2.1 Effect of Normal Load Onspecific Wear Rate and Coefficient of Friction

The influence of load on specific wear rate of SiC/ MD reinforced based Al7075 alloy composite are employed in Fig. 5. Wear steady state wear experiments of SM alloy composites are conducted on five distinct loads like (10, 20, 30, 40 and 50 N) and other two variables are taken as constant sliding velocity (0.9 m/s) and sliding distance of 500 m. It is noticed thatincrease in specific wear ratewithrisein weight percentage of SiC/MD content. The wear rate of SM alloy composites isgreater for SM-08 whiles SM-80 alloy composite of wear rate is lower. Therefore, it noticed the wear rate of compositesorder as SM-08 > SM-26 > SM-44 > SM-62 > SM-80. It concluded, the wear rate of composite enhances with enhance in variation of normal load. The rise in wear rate due to the wear resistance capacity of SM alloy composite is very poor at all respective load conditions. Hence, it might be

Table 5 Response table for S/N ratios (smaller is better)

level	Normal load (N)	Filler content (wt.%)	Sliding velocity (m/s)	Sliding distance (m)
1	31.72	38.54	20.16	37.67
2	28.18	30.84	26.30	24.75
3	27.20	28.24	24.55	26.55
4	25.24	19.91	32.05	22.86
5	23.74	20.55	33.27	21.67
Delta	8.88	20.64	13.11	16.00
Rank	4	1	3	2

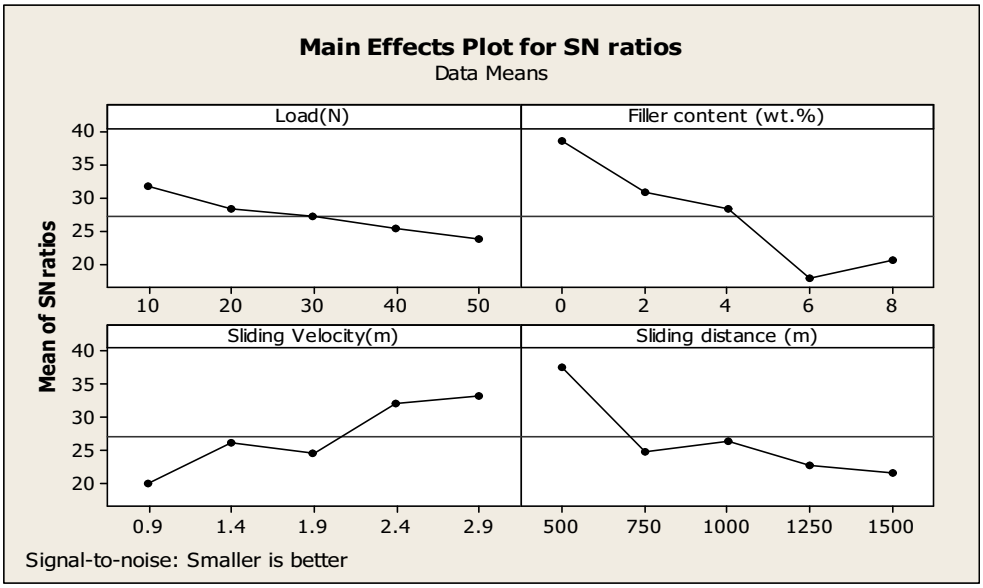

Fig. 9 Effect of control factors for SN ratios

that the hardness of SM alloy composite reduces with increase in normal load and also generates the more porosity of fabrication of new designed SM alloy composite [6, 13].Thus, This may be attributed that the specific wear rate increases with increasing load due to severe plastic deformation of contact asperities across pin-disc interface resulting into higher instant flash temperature that results in material softening and promotes wear via fracture-mechanism.The wear particles at the interface may further accelerate wear rate via three-body abrasion. Further, the mechanism of formation-deformation-destruction-reformation of tribolayer having solid lubricant graphite particulates may causes gradual increase of specific wear rate rather than sharp rates. [38]. The relation between normal load and coefficient of friction of SM alloy composites are illustrated in Fig. 6. It is noticed that the coefficient of friction improves with increment in normal load. Hence the coefficient of friction of SM alloy order as SM-44 < SM-62 < SM-44 < SM-26 < SM-08. Therefore, increased in coefficient of friction with increment in normal load due to the higher plastic deformation and in sliding wear test, debris particles come on disk surface then increase in friction coefficient also. Hence, the coefficient of friction value increases owing to cracking, hard debris and plough mechanism action works on disk surface of composite[6, 20].

Table 6 Analysis of variance for S/N ratios of wear rate

Source	DF	Seq SS	Adj SS	Adj MS	F	P	P (%)
Normal load	4	185.9	166.7	41.7	0.37	0.825	5.05
Filler content	4	1367.8	1228.1	307.0	2.72	0.107	36.94
Sliding velocity	4	644.2	546.1	136.5	1.21	0.379	17.39
Sliding distance	4	600.5	600.5	150.1	1.33	0.338	16.21
Error	8	904.0	904.0	113.0			24.41
Total	24	3702.4					100

S = 10.6299 R-Sq = 75.58% R-Sq (adj) = 26.75%

3.2.2 Effect of Sliding Velocity on Specific Wear Rate and Coefficient of Friction

Influence of sliding velocity on wear rate of SiC/MD reinforced with 7075 alloy composite is depicted in Fig. 7. The wear experiment was performed on the pin on disk tribo-meter apparatus and are taken as different sliding velocity (0.9–2.9 m/s), Normal load (10 N) and sliding distance (500 m). It is noticed that increment in specific wear rate of composite is lower at the initially stage (0.9 m/s); after that the wear rate of composite are suddenly accelerated range from (1.9–2.9 m/s). It is seen that the wear rate of composite shows higher for SM-08 while SM-80 wear rate of composite is lower. Hence, the specific wear rate order is SM-08 > SM-26 > SM-44 > SM-62 > SM-80. Increase in wear rate due to increment in hardness of SM alloy composite. It may be that the wear rate of SM alloy composite increases due to it generates the higher porosity in fabricated composite and the poor interfacial bonding between matrix alloy and SiC content then increase in specific wear rate of composite [39].The Fig. 8 depicts the relationship between sliding velocity (0.9–2.4 m/s) and Coefficient-of- friction of SM alloy composites. The friction of coefficient enhances with increment (step of 2 wt.% of SiC/MD) in weight percentage of SiC/MD (0–8 wt.%) content. It was noticed that increase in coefficient of friction with an increment in sliding velocity (0.9–2.9 m/s) of SM alloy composite. It is seen that the COF value is lower (range from 0.25 to 4.2) at a lower sliding velocity (0.9 m/s-) after that the COF value reaches for higher (0.54) at higher sliding velocity (2.9 m/s) of composite. This may be attributed that increment in Coefficient of friction was increased due to

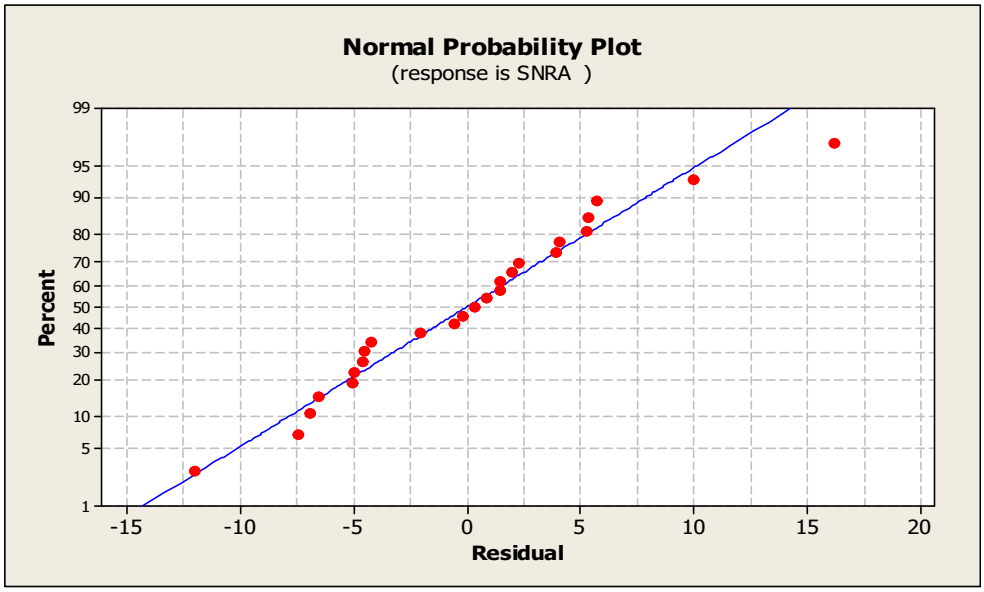

Fig. 10 Effect of control factors on residual and percentage

the unbreakable asperities action on cutting toolsand hard asperities surface of alloy composite. Hence, the Coefficient of friction order is SM-80 < SM-62 < SM-44 < SM-26 < SM-08. Hence, COF enhances due to the plastic deformation in during sliding steady state wear experimental mechanism [6, 23, 24].This may be attributed specific wear rate increases with increasing sliding velocity due to the formation of active thin self-lubricated tribo-layer having solid lubricant graphite particulates whose thickness development might increases with increase in interfacial flash temperature between pin on disc surfaces. [5, 38].

3.3 Taguchi Design of Experiment and ANOVA Analysis

The Taguchi Method of SM alloy composite is used as a scientific optimization tool for measuring robustness and Signal/ Noise ratio is a very important factor in design of parametric. In this technique, the term "signal" indicates the need target, i.e. wear rate of composite and another term "noise" represents the undesirable value. The S/N ratio experimental results are listed in Tables 4 and 5. The entire average mean of the S/N ratio experimental results of SM alloy composite is 27.19 dB respectively. Taguchi experimental results are analyzed through MINITAB 17 software. First any test results are prepared to use a mathematical model as a forecast for determinationof model performance, the suitable interactions between the level and parameters should be considered. Hence, the interaction effect is analyzed by using the factorial parametric design model. The influence of control factors on wear rate are presented in Fig. 9. The significant order of control parameter of a SM alloy composite is reinforcement (R) > Sliding distance (SD) > sliding velocity (V) > Normal load (NL) [20, 24].

The ANOVA results of SM alloy composites are performed for Taguchi L25 DOE and are listed in Table 6. The ANOVA results aid to compute how much percentage contribution each control factor in parametric design of composite i.e. particular wear rate. The P-test indicates a percentage contribution in production for an individual factor. Filler content [$P = 0.107$] < Sliding velocity [$P = 0.338$] < Sliding distance [$P = 0.371$] < Normal load [$P = 0.825$], and are provided in the order of importance of variables. The effect of control factor on residual and percentage is shown in Fig. 10.

3.4 Taguchi Confirmation Test

The confirmation of Taguchi experiment is performed to compare the authenticity of the 95% Significance level in Taguchi design (Table 4). For this condition the test is conducted to experimentally and predicts the specific wear rate via using the MINITAB software. Therefore, the error estimates

Table 7 The error evaluated by using the Taguchi confirmation test

Optimum working parameter Prediction(P_t)		Error Experimental(Exp.)	
	$\overline{A_2}\,\overline{B_2}\,\overline{C_3}\,\overline{D_1}$	$\overline{A_2}\,\overline{B_2}\,\overline{C_3}\,\overline{D1}$	%
Level S/N ratio for wear rate (dB)	56.16	52.84	3.32

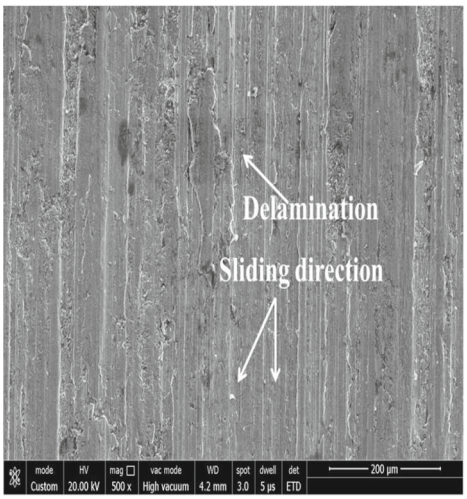

(a) SM-08 at 10 N

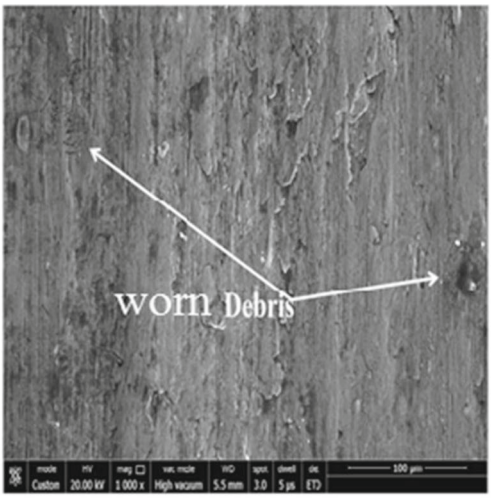

(b) SM-26 at 20 N

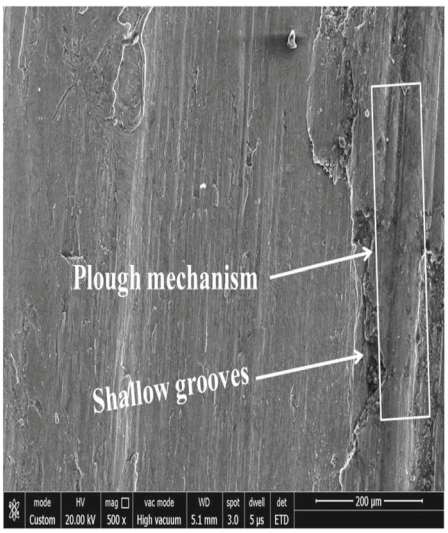

(c) SM-44 at 30 N

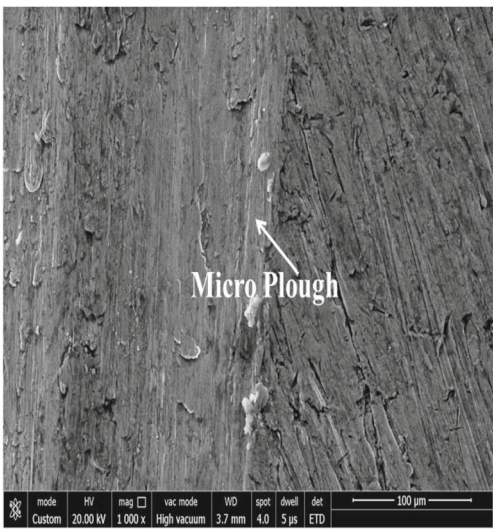

(d) SM-62 at 40 N

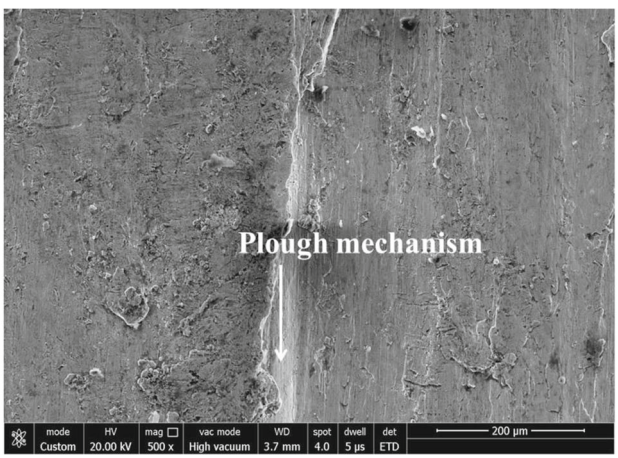

(e) SM-80 at 50 N

Fig. 11 SEM micrograph. (**a**) SM-08 at 10 N (**b**) SM-26 at 20 N (**c**) SM-44 at 30 N (**d**) SM-62 at 40 N (**e**) SM-80 at 50 N

Table 8 Performance criteria and their implications

Sr. No.	Performance criteria	Implications
1.	Compressiv Strength (MPa)	Higher
2.	Flexural Strengt(MPa)	Higher
3.	Impact Strength(J)	Higher
4.	Hardnss (HV)	Higher
5.	Density (g/cc)	Lower
6.	Void content	Lower
7.	Specific wear rate (mm3/N-m)	Lower
8.	COF	Lower

Table 10 Weight of criterion measured by entropy method

Criteria	Ej	ψj	Wj
C1	0.999977434	2.25661E-05	0.185957166
C2	0.901361586	0.098638414	0.530436205
C3	0.995678	0.004322	0.008148
C4	0.999197382	0.000802618	0.001513128
C5	0.638951473	0.361048527	0.680663431
C6	0.98466	0.01534	0.02892
C7	0.9809993	0.0190007	0.035821
C8	0.96874136	0.03125864	0.05893007

between the test data and predict data, compute the error value should be accepted up to 5%. A confirmation test is done by conducting a random test in a group of parameter settings $\overline{A_2}\ \overline{B_2}\ \overline{C_3}\ \overline{D_1}$ to forecast the data of wear rate. The computed S/N ratio for wear rate could be computed via using Eq. 13

$$p = p_n + \sum_{i=1}^{m}(p_i - p_n) \tag{13}$$

where, P_n denotes the best level for S/N ratio; m denotes the no. of factors that influence the quality property; p_i indicates the S/N ratio for each factor at best level. Thus, the Predictive level of $\overline{A_2}\ \overline{B_2}\ \overline{C_3}\ \overline{D_1}$computed via Eq. 14.

$$p = \overline{z} + (\overline{A}_2 - Z) + (B_2 - Z) + (C_3 - Z) + (D_1 - Z) \tag{14}$$

where p represents predict the best value for new composite, z denotes the entire average of the experiment.

The new set of parameter levels $\overline{A_2}\ \overline{B_2}\ \overline{C_3}\ \overline{D_1}$(Load = 40, Filler content = 0 weights of percentage; 2.4 m/s of sliding velocity; sliding distance of 1250 m) are utilized to predict values of wear rate via Eq. 1 and computed the forecast value of S/N ratio is 56.16 dB while 52.84 dB for experimental values of S/N ratio. The estimation error value is 3.11% for S/N ratio and listed in Table 7. Thus, the error may be reduced due to increase in experimental trials.

3.5 SEM Micrograph Studies

The wear surface morphology studies of SM alloy samples were analysis by using electron microscopy in order to understand the underplaying wear mechanism of composite responsible for maximum wear surface damages in the investigated alloy composite.The micrograph studies of SiC/MD reinforced filled 7075 aluminum alloy composite specimens for steady state wear test condition like (Taguchi DOE; L25 orthogonal array) at changing normal load (10-50 N) are presented in Fig. 11a-e. As evident, SM-44 alloy composites show good mechanical properties like lowest voids fraction, maximum strengths etc., Figs. 3 and 4. The Fig. 11a shows the unfilled micro graph of a SM alloy composite of wear rate is 0.005268 mm^3/Nm at Level 1; Table 3. SEM micro graph shows the sliding direction, delamination occurs at lower load of 10 N and lower sliding velocity of 0.5 m/s. Delamination might be occurred owing to less frictional heating between the interfaces of disk and Pin shape materials and also larger quantity of material is removed at the interface of the material [6].

The Fig. 11b shows SEM micrographs that wear debris particles are generated with increment in a load of SM alloy composite. It may be attributed that wear debris particles occur due to the heating material surface at the interface and loss of wear particulates [23]. Figure 11c, d and e shows the plough mechanism, shallow grooves and micro plough generated due to heavy plastic deformation of the material In the sliding steady wear test, two metal piece surfaces are rubbed together as friction is generated at interface of metal surface softening which might further wear particles to loss and create shallow groves and delamination [13, 20]. Similar results are reported by various researchers [31, 34, 37 and 38].

Table 9 Decision matrix

Criteria s→ Alternatives ↓	C1	C2	C3	C4	C5	C6	C7	C8
A1	2.84	1.8	52	400	245	9	0.003	0.014
A2	2.83	0.7	55	440	275	10	0.0014	0.023
A3	2.86	1.9	59	535	335	12	0.0019	0.025
A4	2.87	1.92	65	645	255	14	0.0025	0.028
A5	2.88	1.93	72	665	215	17	0.0029	0.034

Table 11 αi, βi, Ω values and ranking of composites

Composite designation	αi	βi	Ω	Rank
SM-08	0.557726	0.272265	0.219108	2
SM-26	0.964369	0.530436	0.835528	4
SM-44	0.978825	0.680663	1	5
SM-62	0.406872	0.185957	0	1
SM-80	0.660916	0.421318	0.459964	3

3.6 Ranking Analysis Using Hybrid Entropy –VIKOR Method

In various sector applications (like automobile and aerospace) material performance are analyzed via hybrid Entropy – VIKOR Method. The important criteria are hardness, density, void content,compressive strength, impact strength and flexural strength and specific wear rate. The maximum value of characteristics like hardness, compressive strength, impact strength and flexural strength are desirable (benefit criteria), while for minimum value of other properties like density, specific wear rate and coefficient of friction are chosen (cost criteria). Hence, to select the best composition by considering all criterions; hybrid Entropy –VIKOR method was implemented. [20–24]

Table 8 shows the performance criteria and their implication and Table 9 shows the decision matrix of composite Eq. 5). The weight of the criterionswas computed by using Eqs. 6 and Eq. 7 and The utility value measure, regret value and VIKOR method were calculated by using Eqs. 10, 11 and 12 and alternatives with a minimum value of VIKOR index (Table 10) were taken as the best alternatives. Table 11 shows that the maximum value is 1 for SM-44 alloy composite while the minimum value of composite is 0 for SM-62. Hence, the composition of SM-62 alloy composite was considered as the best material performance for tribological application. Similar results are reported by various scientists/ researchers. [25–39].

4 Conclusions

The significant outcomes from this research work are:

1. The both density of SM alloy composites is taken the range of ~2.89–2,96and ~ 2.84–2.88 g/cc while voids content are taken the range of ~1.73–2.70%.
2. Enhance in addition of SiC/MD increase the compressive strength, hardness and impact strength and void content while flexural strength reduces for alloy composite.
3. The wear rate of composite increase with increment in load (10–50 N) condition and it is observed that the wear rate of order is SM-08 > SM-26 > SM-44 > SM-62 > SM-80. The COF value improves with increment in load and obtain the COF order as SM-80 < SM-62 < SM-44 < SM-26 < SM-08.
4. The wear rate of composite increase with increase in sliding velocity (0.9–2.9 m/s) condition and it is noticed that the wear rate of the composites order as SM-08 > SM-26 > SM-44 > SM-62 > SM-80.The COF value improves with increment in load and obtain the COF order as SM-80 < SM-62 < SM-44 < SM-26 < SM-08.
5. The filler content parameter dominates other parameters under specific wear rate investigation adopting Taguchi design of experiment method and the ranking of composition are analyzed using the hybrd Entropy -VIKOR method.
6. The hybrid ENTROPY-VIKOR techniques analysis reveals SM-62 alloy composite shows better improved overall performance relative to others. This is in-line with the subjective analysis. Such decision-making methods may prove helpful in making material selection or ranking.
7. The SEM micrograph analysis revealed that the damaged, worn surface examination through the wear mechanism of the SM alloy composite.

Acknowledgments The authors acknowledged the characterization facilities and other infrastructural support given by the Advanced Research Lab for Tribology and Material Research Centre of Malaviya National Institute of Technology Jaipur.

Author Contributions Ashiwani Kumar: Conceptualization, Methodology, experimentation, Mukesh Kumar: Writing- Reviewing and Editing, Bhavana Pandey: Writing- Original draft preparation.

Funding No funding to declare.

Data Availability Additional data available on reasonable request by email to the corresponding author.

Declarations

Conflict of Interests No potential conflicts of interest concerning the research, authorship, and publication of these articles has been declared by the authors.

Consent to Participate The author's consented to participate in this journal.

Consent Publication The authors consented to publication in this journal.

References

1. Wang DZ, Peng HX, Liu J, Yao CK (1995) Wear behavior and microstructural changes of SiCw-Al composite under unlubricated sliding friction. Wear 184:187–192
2. Harris SJ (1988) Cast metal matrix composites. Mater Sci Technol 4:231–239
3. Chen W, Liu Y, Yang C, Zhu D, Li Y (2014) (SiCp+ Ti)/7075Al hybrid composites with high strength and large plasticity fabricated by squeeze casting. Mater Sci Eng A 609:250–254
4. Prabu SB, Karunamoorthy L (2008) Microstructure-based finite element analysis of failure prediction in particle-reinforced metal–matrix composite. J Mater Process Technol 207:53–62
5. Kumar A, Patnaik A, Bhat IK (2017) Investigation of nickel metal powder on Tribological and Mechanical Properties of al7075Alloy Composites for Gear Material, journal of. Powder Metall 60:371–383
6. Kumar KR, Kiran K, Balaji VS (2017) Micro structural characteristics and mechanical behavior of aluminium metal matrix

composites reinforced with titanium carbides. J Alloys Compd 723: 795–801
7. Kumar KR, Kiran K, Sreebalaji VS (2017) Characterization of mechanical properties of aluminium/tungsten carbide composites. Meas 102:142–149
8. Alhawari KS, Omar MZ, Ghazali MJ, SallehMS MMN (2013) Wear properties of A356/Al2O3 metal matrix composites produced by semisolid processing. Procedia Eng 68:186–192
9. Kiran TS, Kumar MP, Basavarajappa S, ViswanathaBM (2014) Dry sliding wear behavior of heat treated hybrid metal matrix composite using Taguchi techniques. Mater Des 63:294–304
10. Kumar A, Kumar A (2020) Mechanical and dry sliding wear behavior of B_4C and rice husk ash reinforced Al 7075 alloy hybrid composite for armors application by using Taguchi techniques. J Mater Today: Proc 27:2617–2625
11. Bhaskar S, Kumar M, Patnaik A (2019) Application of hybrid AHP-TOPSIS technique in analyzing material performance of silicon carbide ceramic particulate reinforced AA2024 alloy composite. Silicon. 12:1075–1084
12. Kumar M, Kumar A (2020) Application of preference selection index method in performance based ranking of ceramic particulate (SiO2/SiC) reinforced AA2024 composite materials. J Mater Today: Proc 27:2667–2672
13. Singh T, Patnaik P, Fekete G, Chauhan R, Gangil B (2019) Application of hybrid analytical hierarchy process and complex proportional assessment approach for optimal design of brake friction materials. Polym Compos 40:1602–1608
14. Satapathy BK, Majumdar A, Tomar BS (2010) Optimal design of flyash filled composite friction materials using combined analytical hierarchy process and technique for order preference by similarity to ideal solutions approach. Mater Des 31:1937–1944
15. Maniya K, Bhatt MG (2010) A selection of material using a novel type decision –making method: prefence selection index method. Mater Des 31:1785–1789
16. Maniya KD, Batt MG (2011) An alternative multiple attribute decision making methodology for solving optimal facility layout design selection problems. Comput Int Eng 61:542–549
17. Jahan A, Kevin L, Edwards MB (2016) Multi criteria decision analysis for supporting the selection of engineering materials in product design .Butterworth-Heinemann. https://doi.org/10.1016/C2012-0-02834-7
18. Aherwar A, Patnaik A, Bahraminasab M, Singh A (2017) Preliminary evaluations on development of new materials for hip joint femoral head. Mater Des App https://doi.org/10.1177/1464420717714495
19. Kumar M, Kumar R, Tak Y, Meena RK, Sharma N, Kumar A, Parametric optimization and ranking analysis of hybrid epoxy polymer composites based on mechanical, thermo-mechanical and abrasive wear performance(2020)High Perform. Polym https://doi.org/10.1177/0954008320959412
20. Kumar A, Patnaik A, Bhat IK (2019) Tribology analysis of cobalt particulate filled Al 7075 alloy for gear materials: a comparative study. Silicon **11**:1295–1311
21. M.Kumar (2020) Mechanical and Sliding Wear Performance of AA356-Al2O3/SiC/Graphite Alloy Composite Materials: Parametric and Ranking Optimization Using Taguchi DOE and Hybrid AHP-GRA Method, Silicon https://doi.org/10.1007/s12633-020-00544-9
22. Bhaskar S, Kumar M, Patnaik A (2019) Silicon carbide ceramic particulate reinforced AA2024 alloy composite - part I: evaluation of mechanical and sliding tribology performance. Silicon 12:843–865
23. Kumar M, Kumar A (2019) Sliding wear performance of graphite reinforced AA6061 alloy composites for rotor drum/disk applica- tion. Mater Today Proc https://doi.org/10.1016/j.matpr.2019.09.042
24. Ramesh CS, Keshavamurthy R, Channabasappa BH (2010) Friction and wear behavior of Ni–P coated Si3N4 reinforced Al6061 composites. Tribol Int 43:623–634
25. Khorshidi J, Hassani R (2013) A comparative analysis between TOPSIS and PSI method of material selection to achive a desirable combination of strength and workability in Al/SiC composite. Mater Des 52:999–1010
26. Panahi M, Gitinavard H (2018) Evaluating the sustainable mining contractor selection problems: an imprecise last aggregation preference selection method. J. Sustain Min 16:207–2018
27. Mesran I, Tampubolon K, Sianturi RD, Waruwu FT (2017) Determination of education scholarship recipients using preference selection index. Sci Technol 3:230–234
28. Jian SY, Tao SY, Huang XR (2014) Preference selection index method for machine selection in a flexible manufacturing cell. Adv Mater Res 1078:290–293
29. Jha K, Chamoli S, Tayagi YK, Maurya HO (2018) Characterization of biodegradable composites and application of preference selection index method for deciding optimal phase combination. Mater Today Proc 5:3553–3360
30. Dev S, Aherwar A, Patnaik A (2019) Material selection for automotive piston component using entropy-VIKOR method. Silicon 12:155–169. https://doi.org/10.1007/s12633-019-00110-y
31. Moharami A (2020) High-temperature tribological properties of friction stir processed Al-30Mg2Si composites. Mater at High temp https://doi.org/10.1080/09603409.2020.1785792
32. Moharami A, Razaghian A, Babaei B, OO Ojo4 , lapa ´kova MS (2020) Role of Mg2Si particles on mechanical, wear, and corrosion behaviors of friction stir welding of AA6061-T6 and Al-Mg2Si composite. J Compos Mater0(0):1–23 https://doi.org/10.1177/0021998320925528,54
33. Moharami A (2020) Improving the dry sliding wear resistance of as cast cu-10Sn-1P alloy through accumulative back extrusion(ABE). J Mater Res Technol (9)5:10091–10096. https://doi.org/10.1016/j.jmrt.2020.07.022
34. Moharami A, Razaghian A, Paidarc M, Slapakov M, Ojoe OO, Taghiabadib R (2020) Enhancing the mechanical and tribological properties of Mg2Si-rich aluminum alloys by multi-pass friction stir processing. Mater Chem Phys 250:123066. https://doi.org/10.1016/j.matchemphys.2020.123066
35. Moharami A, Razaghia A, Fmamy M, Taghiabadib R (2019) Effect of tool pin profile on the microstructure and Tribological properties of friction stir processed Al-20 wt% Mg2Si composite. J Tribol 141:122202–122201
36. Maharani A, Razaghia A (2020) Corrosion behavior of friction stirs processed. Al–Mg2Si composites Mater Sci Technol 36(18):1922–1929. https://doi.org/10.1080/02670836.2020.1852515
37. Kumar A, Kukshal V, Kiragi (2020) Assessment of Mechanical and Sliding wear performance of Ni particulate filled Al7075 aluminium alloy composite. Mater Today Proc https://doi.org/10.1016/j.matpr.2020.10.556
38. Kumar M, Bhaskar S, Shakyawal NK, Kuma A (2020) Application of preference selection index method in performance (mechanical properties and sliding wear) based ranking of AA2024-Al2O3/SiC alloy composites. Mater Werkst 51:1662–1685. https://doi.org/10.1002/maw.2019001381662
39. Li X, Sosa M, Olofsson U (2015) A pin-on-disc study of the tribology characteristics of sintered versus standard steel gear materials. Wear 340:31–40